Available online www.ejaet.com

European Journal of Advances in Engineering and Technology, 2025, 12(3):48-64

Research Article ISSN: 2394 - 658X

Numerical Assessment of the Mechanical Behaviour of V-shaped Corrugated-core Sandwich Plates Subject to Compressive Loading

Barisua Ebenezer Ngekpe[1], Jepther Burabari[2], Jonathan Webber Ibani[2]

[1]Senior Lecturer, Department of Civil Engineering, Rivers State University, Port Harcourt, Nigeria,
[2]Lecturer Civil Engineering, Rivers State University, Port Harcourt
[2]Masters' degree research student, Department of Civil Engineering, Rivers State University, Port Harcout, Nigeria.

ABSTRACT

This study investigates the mechanical response of steel V-shaped corrugated-core sandwich plates subject to compressive loading using analytical and non-linear static analysis, implemented in ABAQUS/STANDARD software.

Firstly, the critical buckling loads were determined using the classical beam theory and were compared to numerical results. A detail parametric study was carried out to determine the effect of the number of core unit cells on the overall deformation and local collapse behavior of the panels. A user-friendly finite element modeling scheme was formulated to predict critical buckling loads, stress-strain behavior and load-deformation response of the sandwich plate. A three-dimensional analytical rigid body (loading platen) with six degrees of freedom was used as the top face sheets. The corrugated core and the platen were connected using an isotropic hardening, and surface-to-surface hard contact interaction formulation with a friction penalty of 0.15 in Abaqus/Standard.

An 8-node linear brick, reduced integration, hourglass control (C3D8R) element mesh type definition was used in the model to achieve convergence of results. An 8 mm displacement was applied uniformly to the nodes at the apex of the unit cell to simulate compression of the core and by extension, the initial failure modes. The corresponding load-displacement and compressive stress-strain results were obtained. Based on the observations of the five different numbers of unit cells, elastic buckling is the dominant initial failure mode for the steel V-shaped corrugated-core plate, followed by plastic deformation, and subsequent development of plastic hinges are the main failure modes for the steel specimens. A comparison of the critical buckling load resulting from the analytical solution and FE (ABAQUS) simulation confirms that the influence of the number of core unit cells on the behavior of the corrugated core sandwich plate is accurately predicted. The result shows a 5% difference in the critical buckling load of the analytical solution and FE simulation, therefore, depicting an excellent degree of correlation.

Keywords: plate, corrugated -core, buckling, compressive load, V-shaped.

INTRODUCTION

The need for light weight structures with high strength applicable to aircrafts led to the development of corrugated-core sandwich plates (CSP). Development of core materials has continued from the 1940s through to today to reduce the weight of sandwich panels. Balsa, the first core material that was developed, is still in use where weight is not critical such as in cruising yachts and launches (Dan Zenkert, 1995). The late 1940s and 1950s saw the advent of honeycomb core materials, developed primarily for the aerospace industry. Research into the theoretical analysis of sandwich constructions began following World War II with several papers being published between 1945 and 1955 on the strength and stability of sandwich beams, columns, and plates.

Demand for lighter and modular structures has been increasing in recent years due to driving factors in construction projects, such as tight scheduling, labor, management, and overall cost. For instance, reducing the required man-hours is highly favorable for construction companies. The use of prefabricated modular structures leads to a lower number of workers on site and instead, a longer fabrication time in the shop, which is translated to lower costs

(Tehrani et al., 2017). Consequently, the focus of theoretical study has switched over the past years to laminate optimization, with finite element analysis being employed as a design tool for panel analysis problems.

Along with the concept of modular structures, which contributes to easy and fast construction, the weight and performance of the modular structure also play an important role in the overall engineering design and construction regime, while not compromising on the anticipated load-carrying capacity of the structure.

The compression response and subsequent failure modes of corrugated core sandwich plates under lateral compressive loading have been experimentally investigated and numerically analyzed by several researchers in recent years as such:

Lu et al. (2001) investigated the compressive response and failure mechanisms of a corrugated sandwich panel by use of a combined theoretical and experimental approach. In this study, the corrugated specimens were modeled by use of curved beam elements and surface contact elements. Result showed that the panel has the highest compression strength when the initially sinusoidal corrugated core deforms into a square wave pattern. Tian and Lu (2005) optimized the compression design of a corrugated core bonded to either one or two face sheets for minimum weight.

Rejab and Cantwell (2013) conducted a series of experimental and numerical analyses on the compression response and subsequent failure modes of the corrugated core sandwich panels which were made of three different materials: aluminium alloy, glass fibre reinforced plastic (GFRP), and carbon fibre reinforced plastic (CFRP). The corrugated cores were fabricated using a hot press moulding technique and bonded to the face sheets to produce lightweight sandwich plates. Of particular interest in the study was the role of the number of unit cells and the thickness of the cell walls in determining the overall deformation and local collapse response of the plate. They realized that the buckling of the cell walls was the first failure mode in these corrugated structures and increasing the compression loading will result in localized delamination as well as debonding between the skins and the core. Also, they indicated that the predictions offered by numerical models were in good agreement with the experimental data.

Vahidimanesh et al .(2024) investigated the bending response of sandwich panels with novel square and trapezoidal corrugated core made of E-glass fiber reinforced epoxy composites, with both and without polyurethane foaming filling subjected to quasi-static bending loads. Results showed that failure initiation and propagation were governed by matrix cracking in the face sheets and cores, followed by core cell wall buckling and delamination.

Tung Le et al.(2022) studied the mechanical and fracture mechanisms of bio-inspired thin-walled corrugated-core sandwich composite structures made of carbon fiber-reinforced polymer (CFRP) under four-point bending and flatwise compression. Results revealed that fracture mechanisms of specimens in bending tests depend on the fiber -orientations of the core. It was also observed that fracture mechanisms of specimens in bending tests depend on the fiber-orientations of the core. The sandwich specimen with a core angle of 45 degrees exhibited a larger load capacity and bending stiffness than others.

He et al.(2012) carried out semi-analytical method for bending analysis of corrugated -core, honey-comb and X-core sandwich panels, in this study, the discrete geometric nature of the core was considered by treating the core sheet as beams and the sandwich panel as composite structure of plates and beams with proper displacement compatibility. Results obtained were in excellent agreement with that of finite element results reported in literature.

Zeinali et al. (2024) studied the buckling response of a sandwich plate with a trapezoidal corrugated core cut-out using three vibration correlation techniques. The results showed the effectiveness of the method in predicting the buckling load of the structure.

Buckling as a failure is said to have occurred when the configuration of a structure changes under an imposed load. This imposed load could be compression, shear, uniaxial or biaxial. Of critical concern in this failure mode, is to understand when the initial buckling will occur. In some cases, after the initial buckling stage, some load resistance is still retained in the structure, and this is called post-buckling resistance.

Liew et al. (2007) used the mesh-free Galerkin method to analyze the buckling modes of a plate. This method was an alternative to FEA analysis, with the advantage that it could avoid certain problems with element distortion. Nordstrand (1995) using geometrically non-linear finite element analysis, investigated the post-buckling strength of simply supported orthotropic corrugated board panels subjected to edge compressive loading.

Ngekpe, B.E. (2016) applied nonlinear finite element method to study the punching shear in a flat plate. Results bending reinforcement ratios has significant effect on punching shear failure.

Zamanifar et al. (2020) developed a finite strip formulation based on the first-order shear deformation theory to analyze the mechanical and thermal buckling of corrugated core sandwich plates. They investigated the effect of geometric parameters and different boundary conditions on the critical buckling stresses and critical buckling temperature of the corrugated core sandwich plates.

This study presents the analytical and finite element (FE) modeling and analysis of the bending response of a V-shaped corrugated-core plate without face sheets, based on steel for different geometric parameters subject to compressive loading. And also evaluate the variation of number of unit cell and core wall thickness on the bending and buckling strength of the V-shaped corrugated-core sandwich plate.

MATERIALS CHARACTERISTICS AND ANALYTICAL FORMULATION

Material Characteristics

The materials for the face sheets and core shall be structural steel plate of grade S 275 and density 7850Kg/m^3 according to Eurocode 1 (Table A.4 – EN 1991–1–1: 2002). The material coefficients: Young's modulus (E = 200 GPa), shear modulus (G = 81 GPa) and poisson ratio (v = 0.3) according to Eurocode 3 (Section 3.2.6 – EN 1993-1-1:2005). The nominal values of yield strength (fy) and ultimate tensile strength (fu) are 275 N/mm^2 and 430 N/mm^2 (Table 1 & 2 - EN 1993-1-1:2005).

Table 1: Material properties used to analyze the steel corrugated-core sandwich plate

Properties of Steel with Isotropic Hardening		
Property	**Symbol**	**Value**
Density	*P*	7850 Kg/m^3
Young's Modulus	*E*	200 GPa
Poisson's ratio	*v*	0.3

Table 2: Plastic yield stress, MPa/Plastic strain ($\sigma_y/\varepsilon_{pl}$)

251/0	264/0.024	295/0.049	316/0.074
326/0.099	334/0.124	336/0.149	339/0.174

Source:
http://help.3ds.com/2019/english/dssimulia_established/SIMAINPRefResources/erode_material.inp?ContextScope=all

Analytical Formulation

The corrugated-core geometry is defined by a repeating arrangement of unit cells, which are determined by a set of geometric parameters. In this study, the unit cell is based on a triangular profile (V-shaped) and the corrugated specimens consist of several repetitions of an identical unit cell and face sheets (skin) as shown in Figure 1 below.

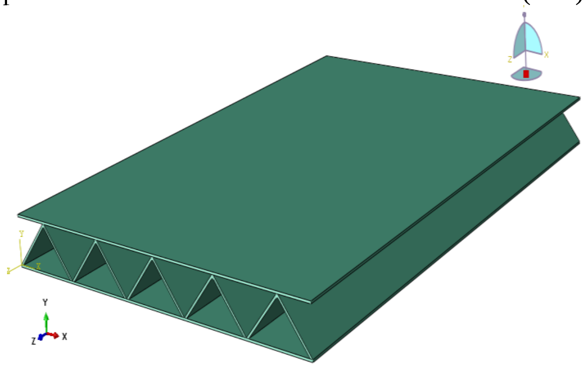

Figure 1: Typical V-shape profile of a corrugated-core sandwich plate.

The geometric parameters are identified in Figure 2.

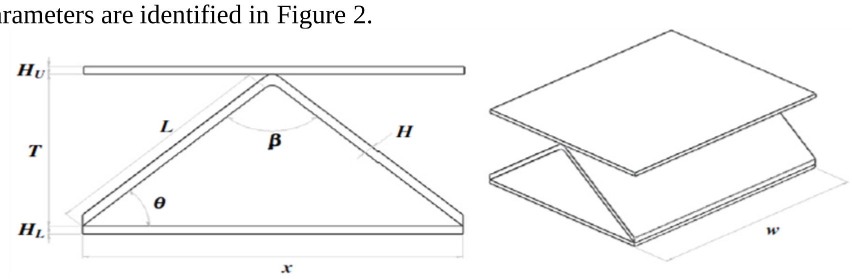

Figure 2: Unit cell geometry of a corrugated-core sandwich plate with V-shape profile. (Rejab and cantwell, 2013)

The parameters are defined as follows:
θ and β are the internal angles of a unit cell in the corrugated-core sandwich panel
T is the height of the core
H_s is the overall height of the sandwich panel
H_u and H_L are the upper and lower thicknesses of the skins, respectively
H is the average thickness of the inclined core member i.e. the wall thickness
x is the width of the core specimen
w is the length of a core specimen.

L is the length of the inclined core member

The responses of the corrugated-core sandwich panels under compression loading and varied geometric parameters are modeled using the ABAQUS/Standard finite element software package. The various results from the analytical simulation, based on the classical beam theory and FE models are tabulated for each geometrical variation and compared for agreement.

Solution of the Analytical Simulation using the classical beam theory.

For perspective, consider the model of the corrugated-core structure with an applied vertical load as shown in Figure 3a. If the sandwich panel is subjected to a compressive load 5P, then a single cell is subjected to a load P as shown in Figure 3b. Due to the symmetry of the triangular profile, each of the core members can be considered as a cantilever beam subjected to the same axial stretching load N, bending moment M, and shear load R as shown in Figure 3c. Here, the lower end of each core member is fixed.

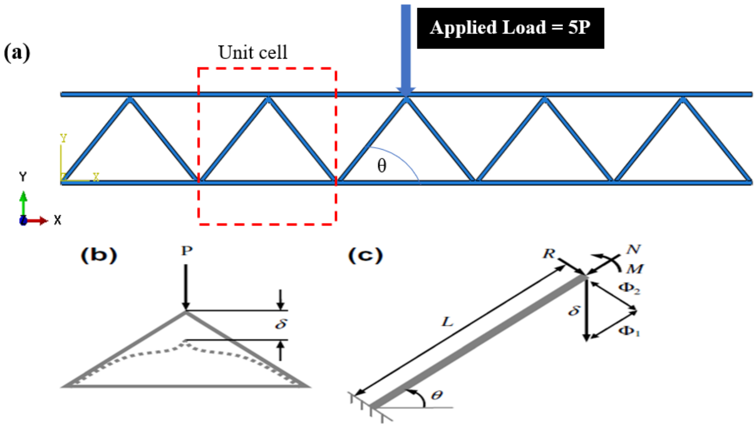

Figure 3: Free-body diagram of (a) five-unit cells (b) a single unit cell (c) a cell wall under compression loading. (Rejab and Cantwell, 2013)

The relative density of the corrugated-core is given as:

$$p^* = \frac{2H}{L\sin 2\theta} \quad (1)$$

Considering the equilibrium of loads in the y-direction, it can be shown that:

$$N\sin\theta + R\cos\theta = \frac{P}{2} \quad (2)$$

and the bending moment M and the shear load R, are related through:

$$\mathbf{M} = \frac{RL}{2} \quad (3)$$

The deformation δ then can be written in terms of the displacement parameters of Φ_1 and Φ_2 as:

$$\Phi_1\sin\theta + \Phi\cos\theta = \delta \quad (4)$$

where the relationship between Φ_1 and Φ_2 is:

$$\Phi_1 = \Phi_2\tan\theta \quad (5)$$

and based on classical beam theory, the relationship between the displacement parameters and the loads acting on the core member can be written as follows:

$$\Phi_1 = \frac{NL}{EA} \quad (6)$$

$$\Phi_2 = \frac{RL}{12EA} \quad (7)$$

where A is the cross-sectional area (A = wH), I, is the second moment of area ($I = wH^3/12$) and E is the Young's modulus of the corrugated-core material. Substituting Eqs. 7, 6, and 5 into Eq. 4, and then solving using Eq. 2, the relationship between the load P and the deformation δ can be shown to be:

$$P = \delta\frac{2EHw(L^2\sin^2\theta + H^2\cos^2\theta)}{L^3} \quad (8)$$

In predicting the strength of the model, Euler buckling and core shear buckling are two possible modes of local elastic buckling in the inclined cell wall under lateral compression load. Here, the Euler buckling load P_E, can be estimated from classical buckling theory as:

$$P_E = \frac{\lambda^2\pi^2 EI}{L^2} \quad (9)$$

where λ is a factor dependent on the boundary conditions. Assuming perfect bonding between the core and the skins, the value of P_E for a corrugated structure here can be expressed as:

$$P_E = \frac{n\lambda^2\pi^2 EwH^3(L^2\sin^2\theta + H^2\cos^2\theta)}{6L^4\sin\theta} \quad (10)$$

SOLUTION OF THE FINITE ELEMENT SIMULATION

Description of Modeling Approach

The responses of the corrugated-core sandwich panels under compression loading and varied geometric parameters are modeled using the ABAQUS/Standard finite element software package. In this work, the face sheets are assumed to carry less significant load, it is therefore sufficient to model the cores without face sheets (skins), whilst applying the appropriate boundary conditions. A three-dimensional analytical rigid body (loading platen) with six degrees of freedom was used as the top face sheet. The core and the platen were connected using an isotropic hardening, and surface-to-surface hard contact interaction formulation with a friction penalty of 0.15 in Abaqus/Standard. The bottom face of the core was modeled perfectly and was fully constrained in all six (6) degrees of freedom. The cores are modeled as a solid element and meshed with 8-node linear brick, reduced integration, and hourglass control (C3D8R) element mesh type resulting in a total mesh element of 750 per unit cell. 8 mm displacement was applied uniformly at a steady step increment to the nodes at the apex of the unit cell to simulate compression of the core. The core length (w = 25 mm), core width (x = 20 mm), and core height (T = 10 mm) are maintained for all the models in this research. The models were used to simulate initial failure and to predict the compression strength and stiffness of the panels. The resulting stress-strain and load-displacement are plotted for each specimen model.

Boundary Conditions

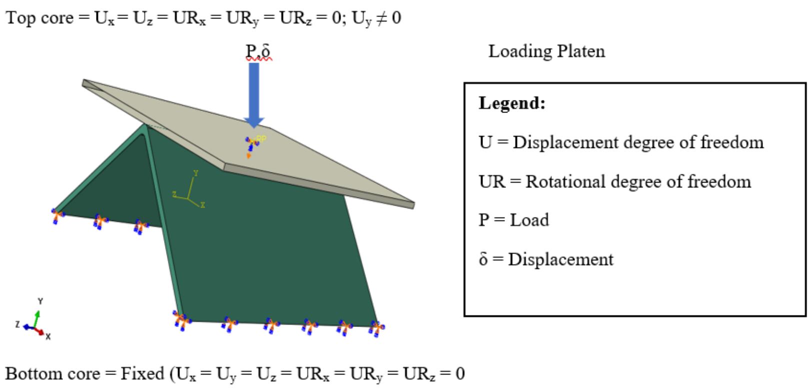

Figure 4: V-shape single-unit cell geometry showing typical boundary conditions

Case I: The Effect of Varying the Number of Core Unit Cells

The effect of varying the number of unit cells on the compressive strength of steel sandwich panels is investigated in ABAQUS/Standard. For this research work, four-unit cells thus: ST1, ST2, ST3, ST4 and ST5 for steel are investigated. See Table 3 below. The cell wall inclination angle is set at 45°, the core wall thickness is assumed to be 0.5 mm and the core height and width is taken as 10 mm and 25 mm respectively

Table 3: Specimen label for the determination of core behaviour for different no. of unit cells

Material	Specimen Core ID				
Steel	ST1	ST2	ST3	ST4	ST5
No of Units	1	2	3	4	5

Contact Interaction in Abaqus/Standard

The cores of the specimen models (ST1, ST2, ST3, ST4, ST5; ST2-0.5, ST2-0.6 and ST2-0.7) are modelled as 3D deformable solid body, while the loading platen is modeled as a 3D analytical rigid solid body. In the interaction module, a rigid body constraint type is assigned to the analytical surface with a reference point (RP) at the center of the analytical body. An isotropic hardening, and surface-to-surface hard contact interaction property with a friction penalty of 0.15 is created and assigned to the loading platen as master surface, and the core as slave surface. Following this interaction, when displacement is applied at the apex node of the cores via the RP of the loading platen, and the cores begins to deform, the contact surfaces of the cores and the loading platen is rigid and impregnable.

Meshing in Abaqus/Standard

The mesh module is used to create the finite element mesh and with the meshing capabilities of ABAQUS/Standard, mesh control, element type and element shape is assigned to the model. A hexagonal (Hex) element shape and 1mm global seeding and sweep mesh technique is assigned to all the specimen models in the study. The standard element library and 3D stress family with linear geometric order is assigned to the models, Consequently, the mesh element type associated with this study is C3D8R: An 8-node linear brick, reduced integration, and hourglass control (C3D8R), with a total mesh element of 750 per unit cell.

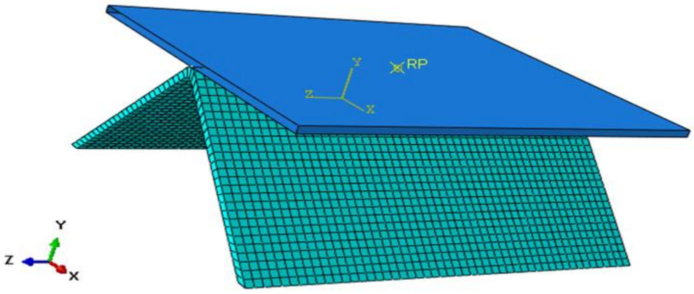

Figure 5: V-shape single-unit cell geometry showing typical element mesh type (C3D8R)

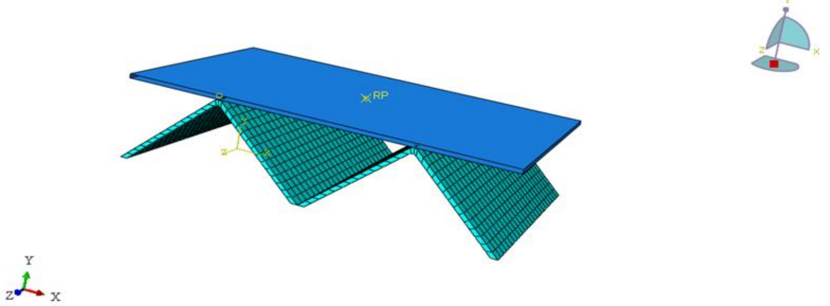

Figure 6: 2-unit cell geometry showing typical element mesh type (C3D8R)

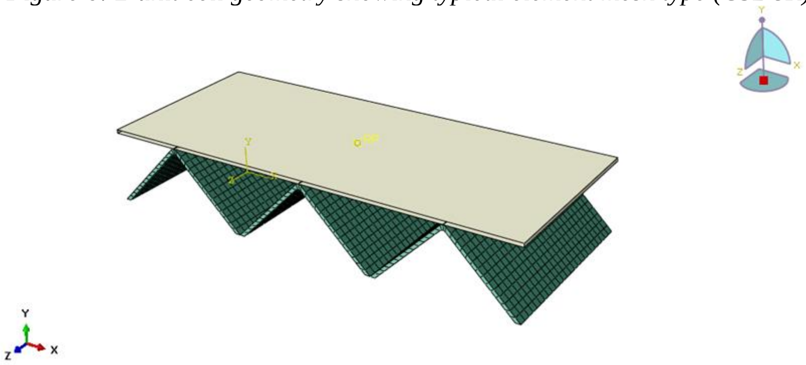

Figure 7: 3-unit cell geometry showing typical element mesh type (C3D8R)

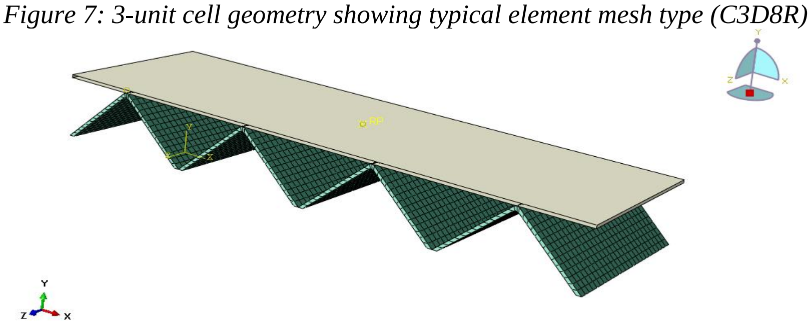

Figure 8: 4-unit cell geometry showing typical element mesh type (C3D8R)

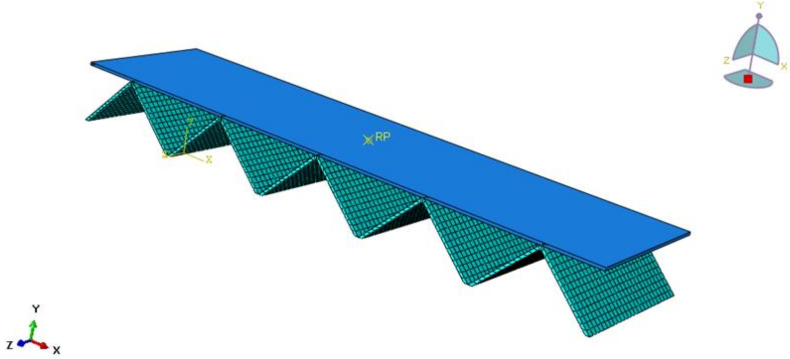

Figure 9: 5-unit cell geometry showing typical element mesh type (C3D8R)

Configuring Solution Step in Abaqus/Standard

The analysis solution to be used in the model is created in the step module. For the V-shaped corrugated-core sandwich plate, the analysis comprises two steps:

• The initial step, in which a boundary condition that constraints the bottom of the cores is applied.

• The general, static general analysis step, in which the displacement/compressive load was applied to the apex node of the cores via the reference point (RP) of the loading platen.

Abaqus generates the initial step as default in the step creation module. The time period it will take ABAQUS/Standard to run the analysis and minimum/maximum number of incrementation is imputed in this module. ABAQUS/Standard updates the solution at the conclusion of each step and inserts it for the following step to take non-linearity into account. The software uses an iterative process to solve the non-linear equilibrium equation by the Newton Raphson numerical technique.

Following the creation of the analysis step, output variables are requested that will form part of the analysis results, either as a field output or history output. The request is made for selected nodes, regions or all elements of the model. The output request for this study are; Von Mises stresses, displacement variable in the y-direction, reaction force in the y-direction. The load-displacement and stress-strain data is obtained by operating on the X-Y data with the combine function in the software.

NUMERICAL RESULTS AND DISCUSSION

CASE I: The Effect of Varying the Number of Core Unit Cells on the Mechanical Behavior of the Corrugated-core Sandwich Panel.

Results of FE Progressive failure model, compressive load-displacement plots, stress-strain relationship and the effects of varying the unit cell of the specimens ST1, ST2, ST3, ST4, and ST5 are presented in Fig 10 – Fig 26.

The regions (I)-(V) shown on the graphs of the progressive failure models of Fig 4.2, 4.6, 4.10, 4.14 and 4.18 represents critical stress - strain points (S22 – stress component in the y-direction and the corresponding E22 – Total strain component in the y-direction) on the specimens (ST1, ST2, ST3, ST4 and ST5) and corresponds to the regions on the compressive stress-compressive strain plot of Fig 10, 13, 16, 19, and 22.

The results of this FE simulation on the steel V-shaped corrugated cores suggests elastic buckling, plastic deformation, and the development of plastic hinges as the main failure modes for the core material.

A comparison of the critical buckling load (Pcr) arising from the analytical solution and FE (ABAQUS) simulation as shown in Table 4, confirms that the influence of the number of core unit cells on the behavior of the corrugated core sandwich plate is accurately predicted. The result shows a 5% difference in the critical buckling load of the analytical solution and FE simulation, therefore, depicting appreciable degree of correlation.

Table 4 Analytical and FE model results of the critical buckling load (Pcr) of ST1 – ST5 test specimens

Specimen Core ID	ST1	ST2	ST3	ST4	ST5
FE (ABAQUS) Critical Buckling Load (P_{cr})- N	906	1811	2659	3552	4502
Analytical Critical Buckling Load (P_{cr})- N	856	1761	2609	3502	4452
Percentage (%) Difference	5.5	5.5	5.5	5.5	5.5

FE analysis models and graphs for ST1:

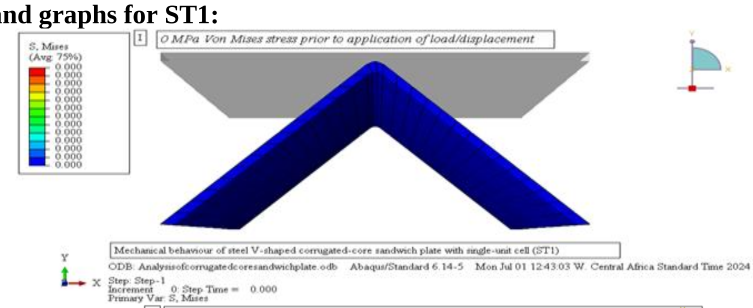

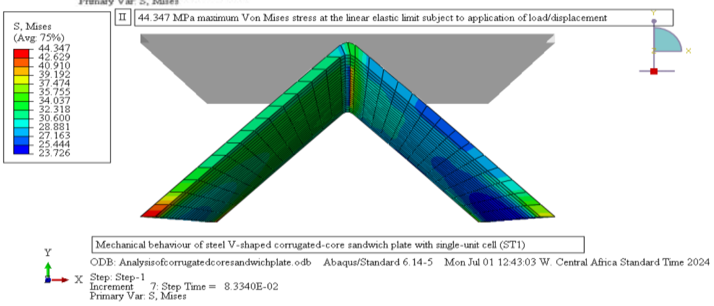

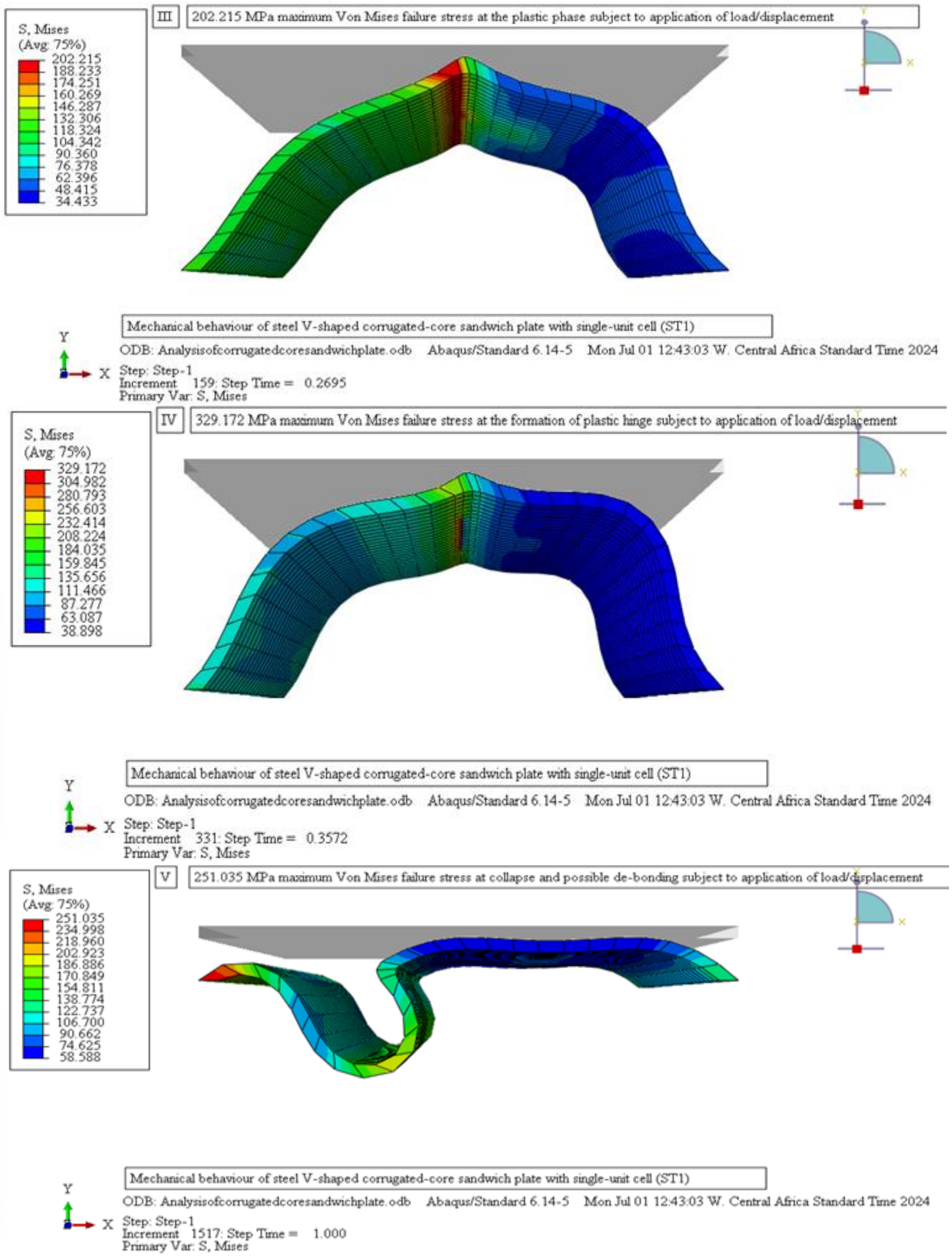

Figure 10: graph of progressive failure development in steel (ST1) single-unit cell

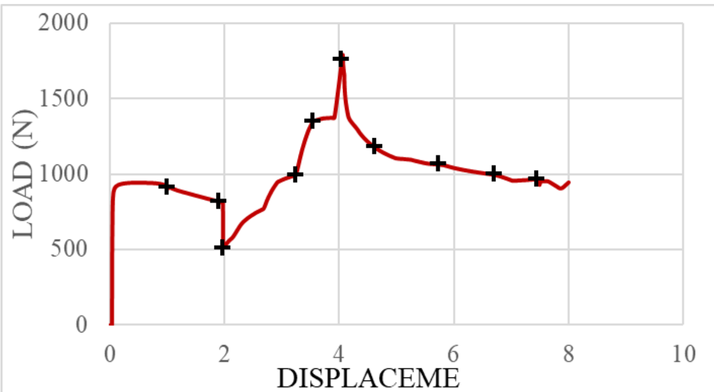

Figure 11: Load-Displacement graph for Steel (ST1) single-unit cell

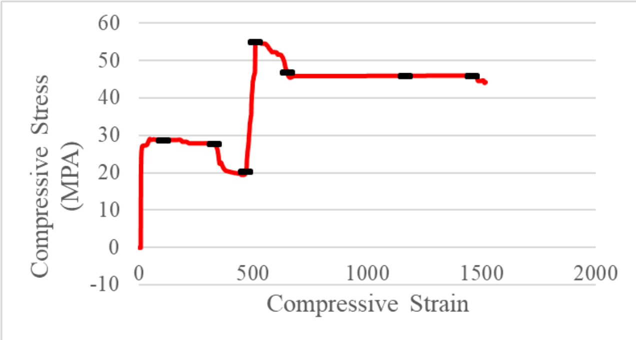

Figure 12: Stress-Strain graph for Steel (ST1) single-unit cell

With reference to the FE result presented in Table 4, progressive failure images of Figure 10, and graphs of Figures 11 and 12, it could be observed that the single-unit (ST1) CSP exhibits ductility with linear elasticity in the region (I) – (II) subject to compressive loading. At point (II), the linear elastic load (critical buckling load Pcr) peaks at 906 N, beyond which the CSP begins to undergo deformation (buckling) under further application of load, as a result of one of the corrugated-core cell walls partially bending after it reached its peak stress. Between region (II) and (III) the load to further deform the core sample drops steadily and reaches the summit 511 N at region (III) as plastic buckling causes the panel to lose stability. Due to interactions between the surfaces of the cell walls and the loading platen, the corrugated core in region (III) - (IV) assumes a trapezoidal shape and the applied stress begins to increase once more and peaks 1760 N at region (IV). Finally, the corrugated core in Region (V) has fully collapsed, which in some cases, results in de-bonding of the cores from the skin at the sample's nodes.

FE analysis models and graphs for ST2:

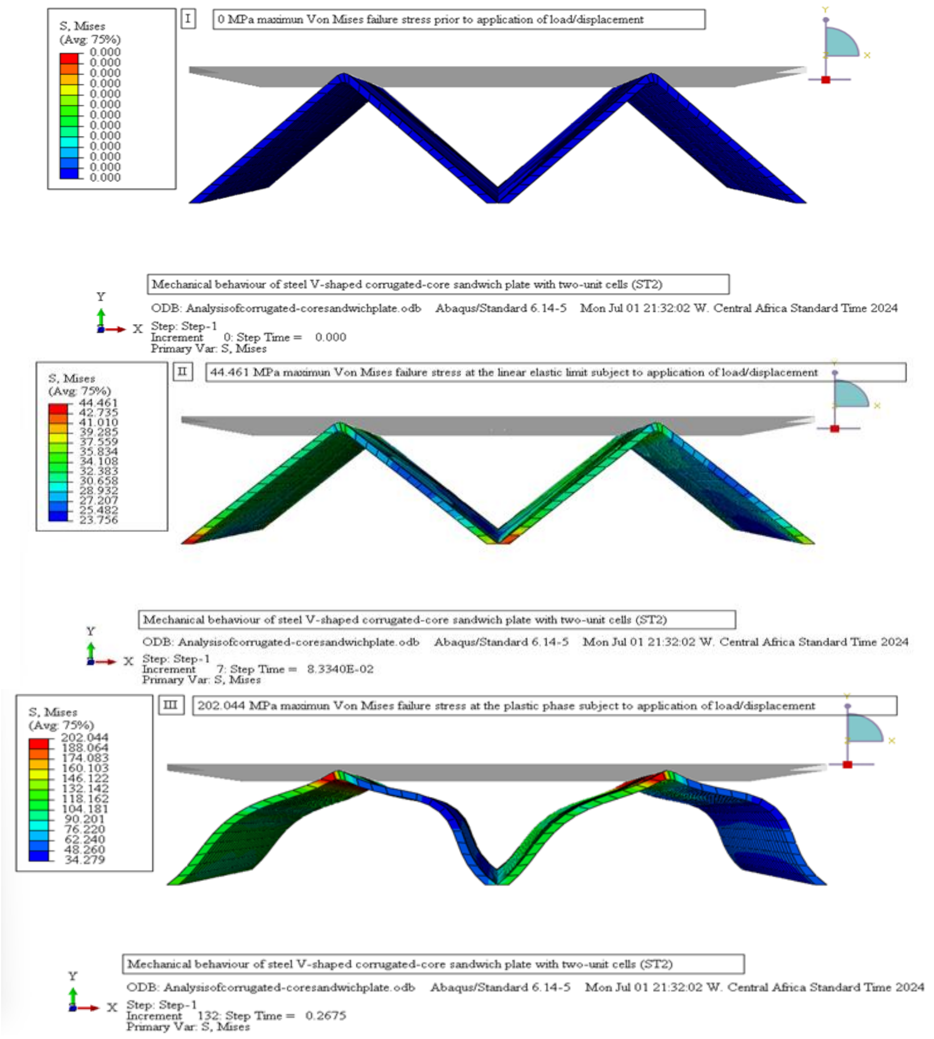

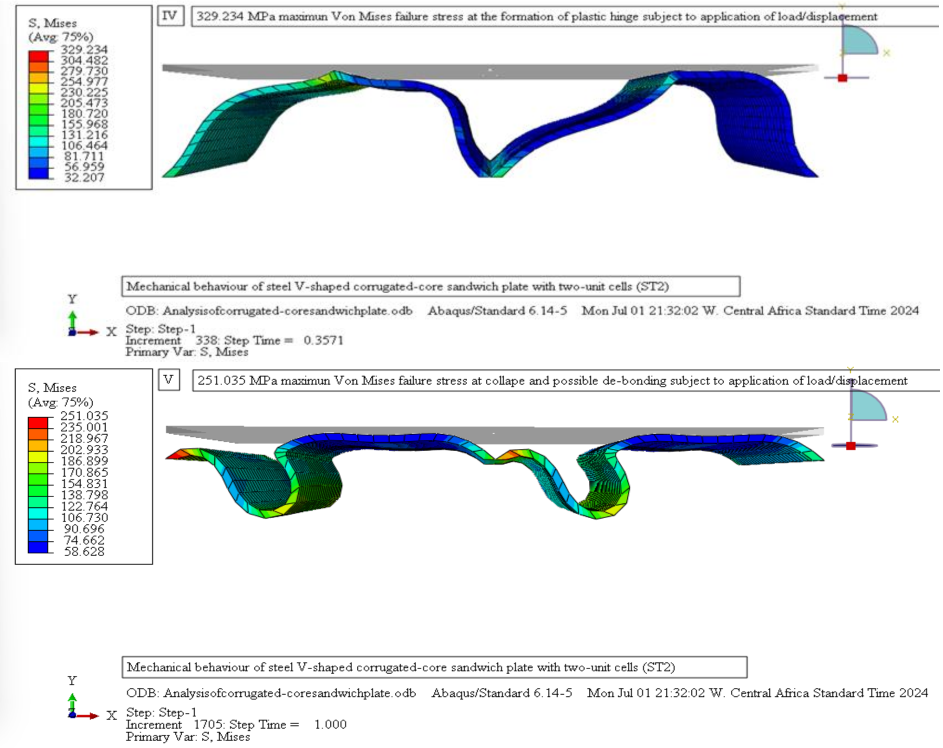

Figure 13: Graph of progressive failure development in steel (ST2) two-unit cell

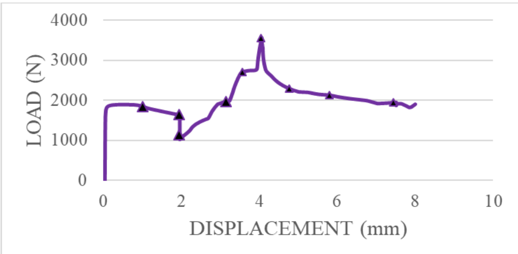

Figure 14: Load-Displacement graph for Steel (ST2) two-unit cell

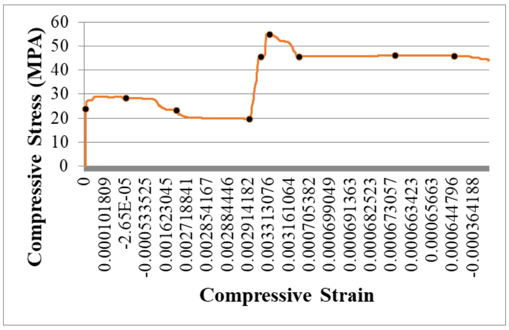

Figure 15: Stress-Strain graph for Steel (ST2) two-unit cell

With reference to the FE result presented in Table 4, progressive failure images of Figure 13, and graphs of Figures 14 and 15, it could be observed that the two-unit (ST2) CSP exhibits ductility with linear elasticity in the region (I) – (II) subject to compressive loading. At point (II), the linear elastic load (critical buckling load Pcr) peaks at 1811 N, beyond which the CSP begins to undergo deformation (buckling) under further application of load, as a result of one of the corrugated-core cell walls partially bending after it reached its peak stress. Between region (II) and (III) the load to further deform the core sample drops steadily and reaches the summit 1045 N at region (III) as plastic buckling causes the panel to lose form and stability. Due to interactions between the surfaces of the core cell walls and the loading platen, the corrugated core in region (III) - (IV) assumes a trapezoidal shape and the applied stress begins to increase once more and peaks 3540 N at region (IV). Finally, the corrugated core in Region (V) has fully collapsed, which in some cases, results in de-bonding of the cores from the skin at the sample's nodes.

FE analysis models and graphs for ST3:

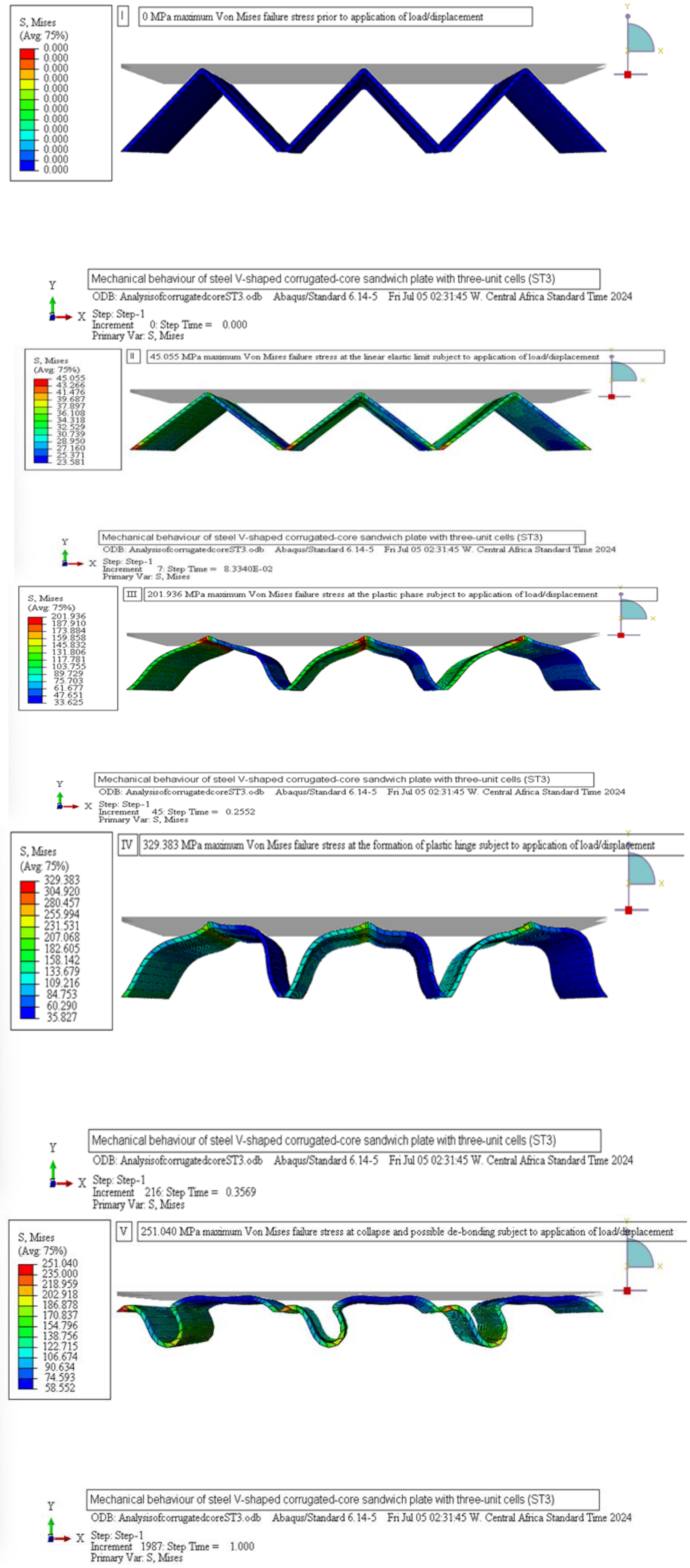

Figure 16: Graph of progressive failure development in steel (ST3) three-unit cell

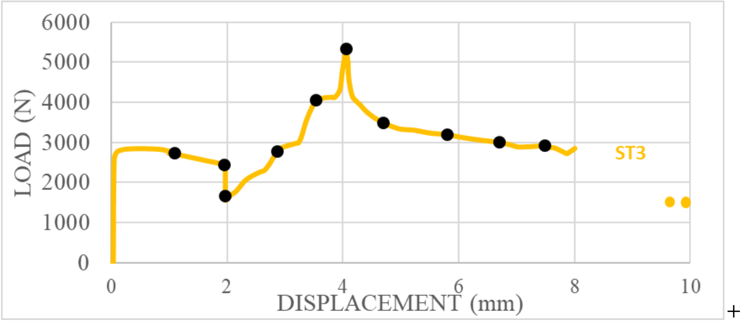

Figure 17: Load-Displacement graph for Steel (ST3) three-unit cell

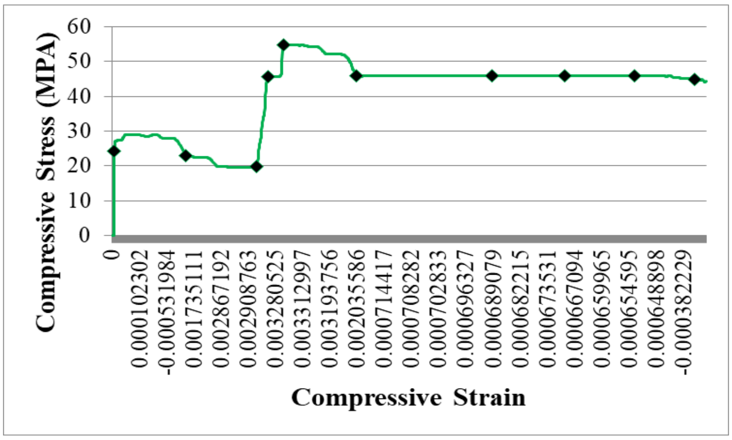

Figure 18: Compressive Stress-Compressive strain graph for Steel (ST3) three-unit cell

With reference to the FE result presented in Table 4., progressive failure images of Figure 16, and graphs of Figures 17 and 18, it could be observed that the three-unit (ST3) CSP exhibits ductility with linear elasticity in the region (I) – (II) subject to compressive loading. At point (II), the linear elastic load (critical buckling load Pcr) peaks at 2659 N, beyond which the CSP begins to undergo deformation (buckling) under further application of load, as a result of one of the corrugated-core cell walls partially bending after it reached its peak stress. Between region (II) and (III) the load to further deform the core sample drops steadily and reaches the summit 1555 N at region (III) as plastic buckling causes the panel to lose form and stability. Due to interactions between the surfaces of the core cell walls and the loading platen, the corrugated core in region (III) - (IV) assumes a trapezoidal shape and the applied stress begins to increase once more and peaks 5335 N at region (IV). Finally, the corrugated core in Region (V) has fully collapsed, which in some cases, results in de-bonding of the cores from the skin at the sample's nodes.

FE analysis models and graphs for ST4:

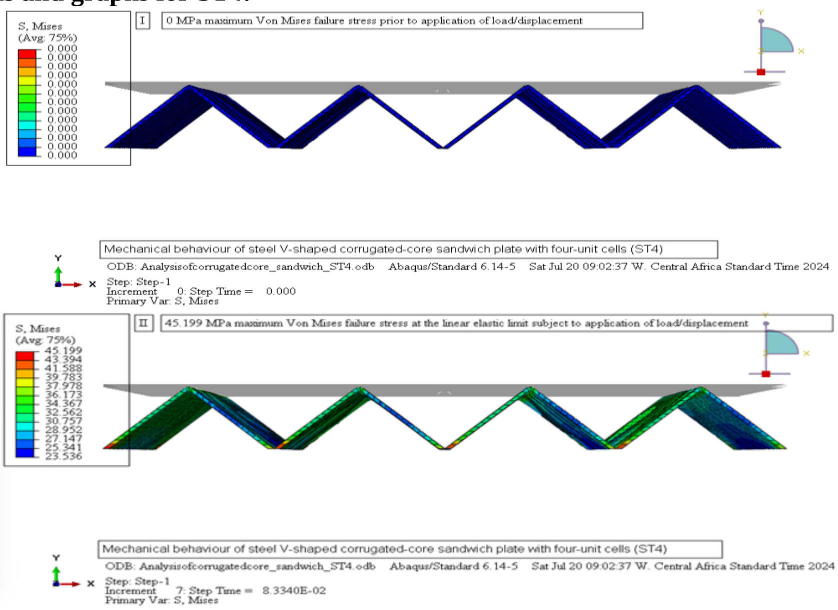

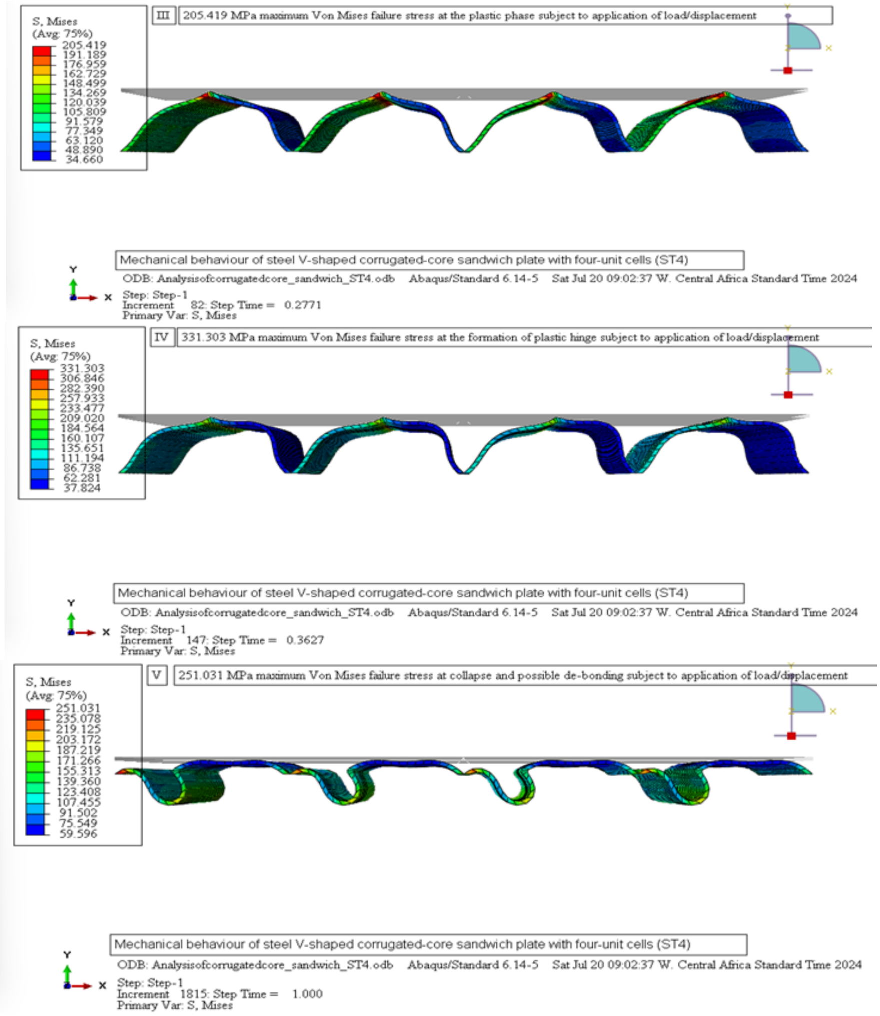

Figure 19: Graph of progressive failure development in steel (ST4) four-unit cell

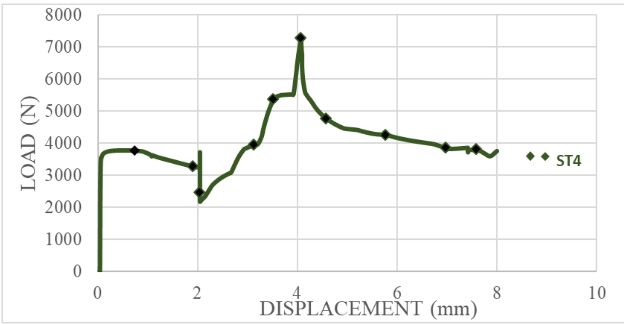

Figure 20: Load-Displacement graph for Steel (ST4) four-unit cell

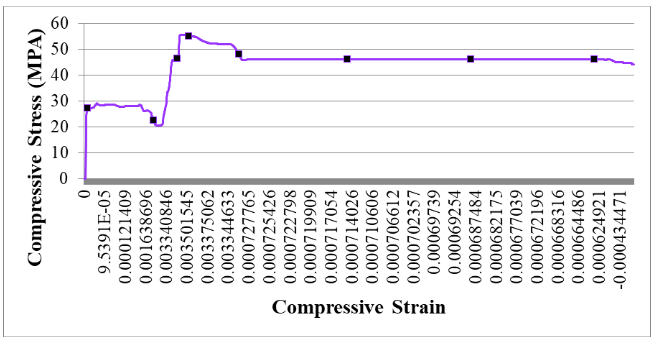

Figure 21: Compressive Stress-Compressive strain graph for Steel (ST4) four-unit cell

With reference to the FE result presented in Table 4., progressive failure images of Figure 19, and graphs of Figures 20 and 21, it could be observed that the four-unit (ST4) CSP exhibits ductility with linear elasticity in the region (I) – (II) subject to compressive loading. At point (II), the linear elastic load (critical buckling load Pcr) peaks at 3552 N, beyond which the CSP begins to undergo deformation (buckling) under further application of load, as a result of one of the corrugated-core cell walls partially bending after it reached its peak stress. Between region (II) and (III) the load to further deform the core sample drops steadily and reaches the summit 2200 N at region (III) as plastic buckling causes the panel to lose form and stability. Due to interactions between the surfaces of the core cell walls and the loading platen, the corrugated core in region (III) - (IV) assumes a trapezoidal shape and the applied stress begins to increase once more and peaks 7265 N at region (IV). Finally, the corrugated core in Region (V) has fully collapsed, which in some cases, results in de-bonding of the cores from the skin at the sample's nodes.

FE analysis models and graphs for ST5:

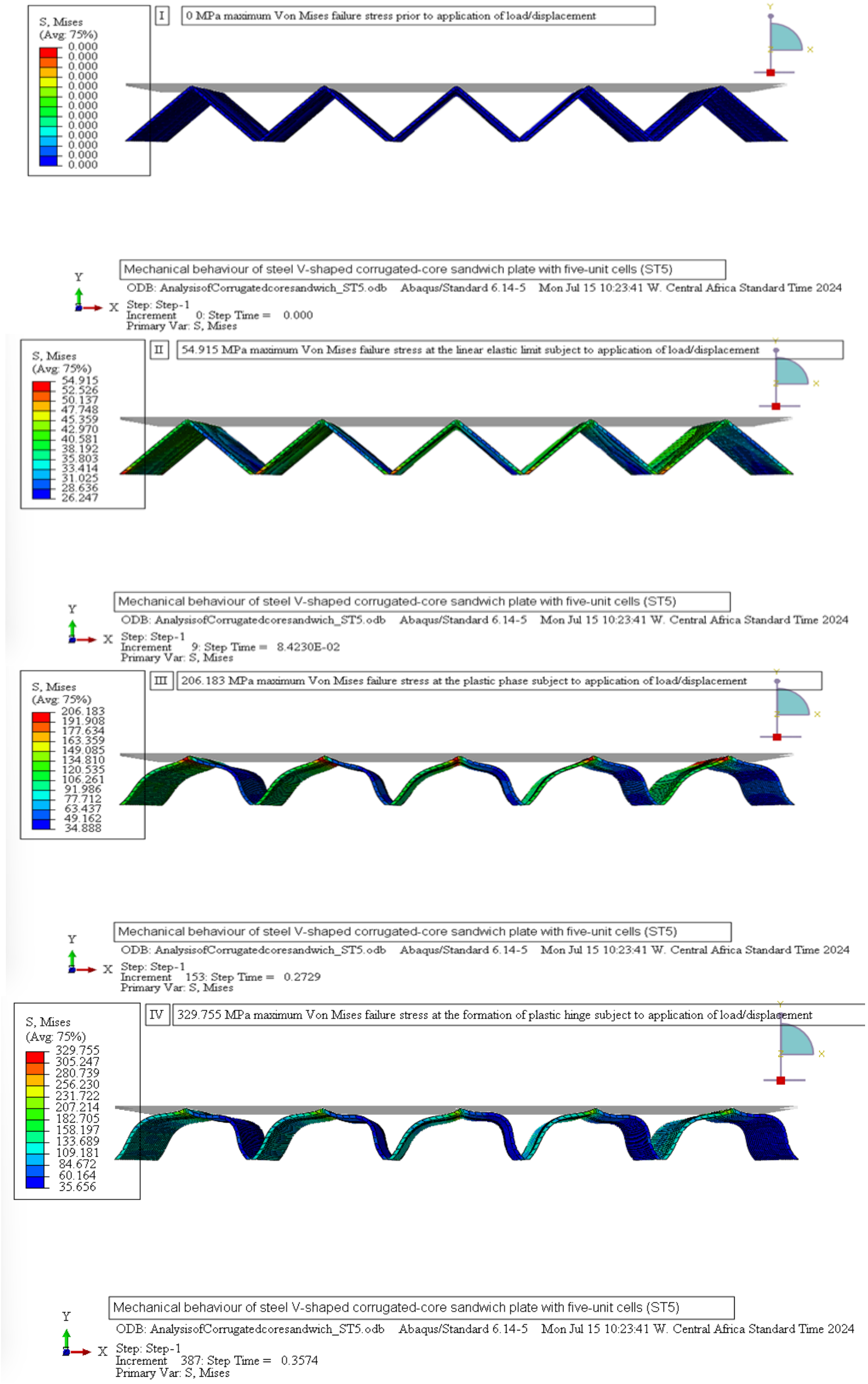

Figure 22: Graph of progressive failure development in steel (ST4) four-unit cell

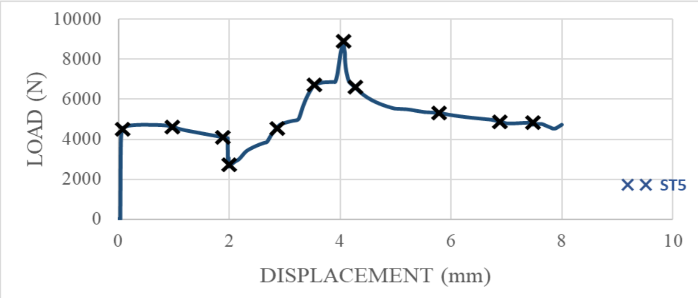

Figure 23: Load-Displacement graph for Steel (ST5) five-unit cell

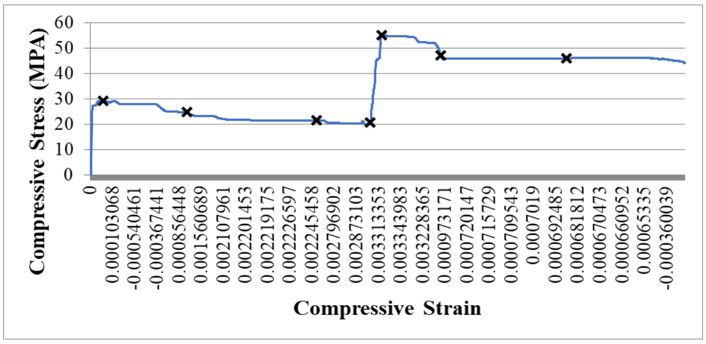

Figure 24: Compressive Stress-Compressive strain graph for Steel (ST5) five-unit cell

With reference to the FE result presented in Table 4, progressive failure images of Figure 22, and graphs of Figures 23 and 24, it could be observed that the five-unit (ST5) CSP exhibits ductility with linear elasticity in the region (I) – (II) subject to compressive loading. At point (II), the linear elastic load (critical buckling load Pcr) peaks at 4502 N, beyond which the CSP begins to undergo deformation (buckling) under further application of load, as a result of one of the corrugated-core cell walls partially bending after it reached its peak stress. Between region (II) and (III) the load to further deform the core sample drops steadily and reaches the summit 2720 N at region (III) as plastic buckling causes the panel to lose form and stability. Due to interactions between the surfaces of the core cell walls and the loading platen, the corrugated core in region (III) - (IV) assumes a trapezoidal shape and the applied stress begins to increase once more and peaks 8930 N at region (IV). Finally, the corrugated core in Region (V) has fully collapsed, which in some cases, results in de-bonding of the cores from the skin at the sample's nodes.

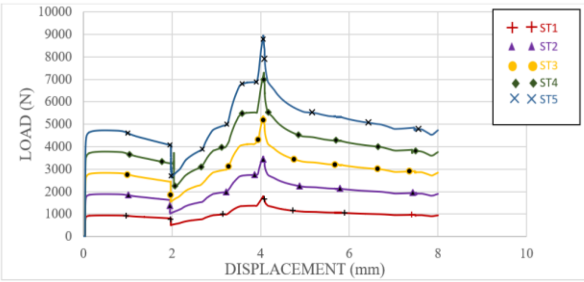

Figure 25: Combined Load-Displacement graph for ST1, ST2. ST3, ST4 and ST5

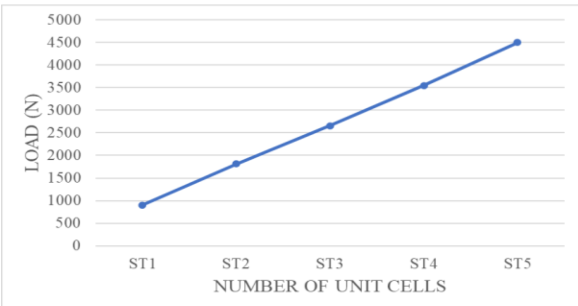

Figure 26: Effect of varying number of unit cells on the compressive load of steel V-shaped corrugated core sandwich plates

Consequent upon the critical buckling load of the test specimens, ST1, ST2, ST3, ST4, and ST5 as shown in Figure 26 above, it is evident that the compressive strength of the steel V-shaped corrugated-core sandwich increases linearly as the number of core unit cell is varied per unit length.

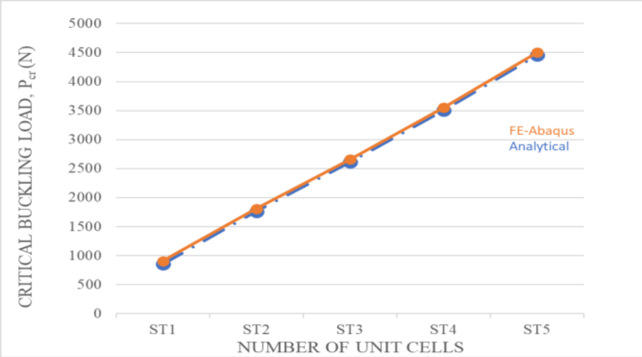

Figure 27: Comparison between Analytical and FE critical buckling load (Pcr) for ST1 – ST5

CONCLUSION

The compressive behaviour and resulting failure mechanisms in steel V-shaped corrugated-cores sandwich plates have been investigated using FE simulation and analytical solution in line with the aims and objectives of this research work. The analytical mechanical buckling analysis of the steel V-shaped corrugated-core sandwich plates was carried out using the classical beam theory. To obtain the mechanical properties of the plate, the walls of the CSP were treated as an equivalent beam with constant height. The effect of geometric parameters such as varying the number of unit cells on the mechanical behavior of corrugated sandwich plates with different boundary conditions subject to static compression loading were investigated. Salient findings are presented as follows:

i. The steel corrugated core sandwich plate exhibits three failure modes; elastic buckling, plastic deformation, and formation of plastic hinges.
ii. The critical buckling load is the peak load within the linear elastic buckling mode (ST1=906N, ST2=1811N, ST3=2659N, ST4=3552N and ST5=4502N) of the corrugated core sandwich plate, which defines the compressive strength of the corrugated core sandwich plate.
iii. An increase in the number of unit cells increases the stiffness properties and in turn, the compressive strength of the core plate. A 50% increase in buckling load between ST1 and ST2, 32% increase between ST2 and ST3, 25% increase between ST3 and ST4 and 21% increase between ST4 and ST5 was recorded.
iv. The result shows a 5.5% difference in the critical buckling load of the analytical solution and FE simulation, therefore depicting excellent degree of correlation.

REFERENCES

[1]. British Standard Institution. BS8110 (1997).
[2]. Dan Zenkert (1995). An introduction to sandwich structures. Student edition
[3]. https://www.diva-portal.org/smash/get/diva2:1366182/FULLTEXT01.pdf
[4]. He, L., Cheng, Y & Liu, J. (2012). Precise bending stress analysis of corrugated-core, honey-comb-core and X-core sandwich panels. Journal of composite structures. 94, 1656-1668.
[5]. Liew, K. M., Peng, L. X., & Kitipornchai, S. (2007). Nonlinear analysis of corrugated plates using a FSDT and a meshfree method. Computer Methods in Applied Mechanics and Engineering, 196(21-24), 2358-2376.
[6]. Lu, T. J. & Zhu, G. (2001). The elastic consent of corrugated board panels. Journals of Composite Materials, 35, 1868-1887.
[7]. Ngekpe, B.E., Ode.T., & Eluozo, S.N. (2016). Application of total-strain crack model in finite social science 6(12), 1-9.
[8]. element analysis for punching shear at edge connection, International Journal of Engineering and
[9]. Nordstand, T., Carlesson, L.A., & Allen, HG. (1995). Transverse shear stiffness of structural core sandwich. Composite Structures, 27, 317-329.
[10]. Rejab, M.R.M., & Cantwell, W.J. (2013). The mechanical behaviour of corrugated core sandwich panels. Composites Part B: Engineering, 47, 267-277.
[11]. Tian, Y. & Lu, T., (2005). Optimal design of compression corrugated panels. Thin-Walled Structures, 43,477-498.
[12]. Tehrani et al. (2017). Parametric study on mechanical response of corrugated-core sandwich panels for bridge decks. Journal of bridge engineering 22(5): 04017002

[13]. Vahidimanesh, B., Farrokhabadi, A & Shahvari, R. et al.(2024). Experimental and numerical investigation of damage in multilayer sandwich panels with square and trapezoidal corrugated cores under quasi-static three-point bending. Journal of engineering structures (318), 1, 118715.

[14]. Zamanifar, H., Sarrami-Foronshani & Azhani, M. (2020). A parametric study on the mechanical and thermal stability of corrugated-core sandwich plates. Journal of structures. 24, 209-226.

[15]. Tung Le, V., Jin, T. & Goo, N.S. (2022). Mechanical behaviours and fracture mechanisms of CFRP sandwich composite structures with bio-inspired thin-walled corrugated cores. Journal of Aerospace science and Technology. 126, 107599.

[16]. Zeinali, M., Rahimi,G & Hasseini, S. (2024). Buckling load optimization of sandwich plates with trapezoidal corrugated core and elliptical cutout using vibration correlation techniques and artificial neural network, experimental and numerical analysis, Journal of thin-walled structures. 200, 111957.